Video Article

Pulling Membrane Nanotubes from Giant Unilamellar Vesicles

Coline Prévost*[1,2,3], Feng-Ching Tsai*[1,4], Patricia Bassereau[1,4], Mijo Simunovic[1,5]

[1]Laboratoire Physico Chimie Curie, Institut Curie, PSL Research University, CNRS UMR168

[2]Department of Genetics and Complex Diseases, T. H. Chan School of Public Health, Harvard Medical School

[3]Department of Cell Biology, Harvard Medical School

[4]Sorbonne Universités, UPMC University Paris 06

[5]Center for Studies in Physics and Biology, The Rockefeller University

*These authors contributed equally

Correspondence to: Patricia Bassereau at patricia.bassereau@curie.fr

URL: https://www.jove.com/video/56086
DOI: doi:10.3791/56086

Keywords: Microbiology, Issue 130, Membrane curvature, membrane nanotube, biophysics, vesicle, optical tweezers, confocal microscopy, curvature sorting, *in vitro* reconstitution, BAR proteins, endocytosis

Date Published: 12/7/2017

Citation: Prévost, C., Tsai, F.C., Bassereau, P., Simunovic, M. Pulling Membrane Nanotubes from Giant Unilamellar Vesicles. *J. Vis. Exp.* (130), e56086, doi:10.3791/56086 (2017).

Abstract

The reshaping of the cell membrane is an integral part of many cellular phenomena, such as endocytosis, trafficking, the formation of filopodia, *etc*. Many different proteins associate with curved membranes because of their ability to sense or induce membrane curvature. Typically, these processes involve a multitude of proteins making them too complex to study quantitatively in the cell. We describe a protocol to reconstitute a curved membrane *in vitro*, mimicking a curved cellular structure, such as the endocytic neck. A giant unilamellar vesicle (GUV) is used as a model of a cell membrane, whose internal pressure and surface tension are controlled with micropipette aspiration. Applying a point pulling force on the GUV using optical tweezers creates a nanotube of high curvature connected to a flat membrane. This method has traditionally been used to measure the fundamental mechanical properties of lipid membranes, such as bending rigidity. In recent years, it has been expanded to study how proteins interact with membrane curvature and the way they affect the shape and the mechanics of membranes. A system combining micromanipulation, microinjection, optical tweezers, and confocal microscopy allows measurement of membrane curvature, membrane tension, and the surface density of proteins, concurrently. From these measurements, many important mechanical and morphological properties of the protein-membrane system can be inferred. In addition, we lay out a protocol of creating GUVs in the presence of physiological salt concentration, and a method of quantifying the surface density of proteins on the membrane from fluorescence intensities of labeled proteins and lipids.

Video Link

The video component of this article can be found at https://www.jove.com/video/56086/

Introduction

Many cellular processes, such as endocytosis, trafficking, the formation of filopodia, infection, *etc.*, are accompanied by a dramatic change in the shape of cell membranes[1,2]. In the cell, a number of proteins participate in these processes by binding to the membrane and altering their shape. The most notable examples are members of the Bin/Amphiphysin/Rvs (BAR) protein family, containing a characteristic intrinsically curved BAR domain[3,4,5,6,7]. Typically, they interact with the membrane by adhering the BAR domain to the surface and, in many cases, also shallowly inserting amphipathic helices into the bilayer. The shape, size, and charge of the BAR domain together with the number of amphipathic helices determines: (1) the direction of membrane curvature (*i.e.*, whether they will induce invaginations or protrusions), and (2) the magnitude of membrane curvature[5,8]. Of note, here positive curvature is defined as the convex side of the curved membrane, *i.e.*, the bulge toward the interacting particle, and negative otherwise. Moreover, quantitative studies of BAR proteins revealed that their effect on the membrane depends on a set of physical parameters: surface density of proteins, membrane tension, and membrane shape (flat *versus* tubular *versus* spherical shape)[7]. Depending on these parameters BAR proteins can: (1) act as sensors of membrane curvature, (2) bend membranes, or (3) induce membrane scission[7].

Due to the sheer number of components involved in membrane reshaping in the cell, studying the quantitative aspects of the phenomena, such as endocytosis, *in vivo* is extremely challenging. *In vitro* reconstitution of minimal components mimicking curved membranes in the cell provides means to gain a mechanistic understanding of how membrane-curving proteins operate. This article describes a protocol to reconstitute a membrane nanotube *in vitro* using micromanipulation, confocal microscopy, and optical tweezers. The approach can be used to study, in a quantitative way, how proteins, lipids, or small molecules interact with curved membranes. Lipid GUVs are used as models of a cell membrane, whose curvature is negligible compared to the size of interacting membrane-curving molecules. They are prepared using the electroformation method[9] in which the vesicles are formed by hydrating a lipid film and swelling it into GUVs under an alternating current (AC)[10]. Most common substrates on which GUVs are grown are either semi-conductive plates coated with indium tin oxide (ITO) or platinum wires (Pt-wires)[11]. In this work, GUVs are grown on Pt-wires as this method has been shown to work much better than the alternative in making GUVs in the presence of

salts in the buffer[12]. Although the electroformation protocol is described here in sufficient detail to reproduce it, we refer the reader to previous articles in which similar and other methods of making GUVs have been described in detail[13,14]. In our hands, electroformation on Pt-wires has successfully yielded GUVs from a mix of synthetic lipids or from natural lipid extracts in a buffer containing ~100 mM NaCl. Furthermore, it was also possible to encapsulate proteins inside GUVs during growth. An example electroformation chamber is shown in **Figure 1A**; it comprises two ~10-cm-long Pt-wires inserted into a holder made from polytetrafluoroethylene (PTFE) that can be sealed on both sides with glass coverslips ~1 - 2 cm apart (**Figure 1A**).

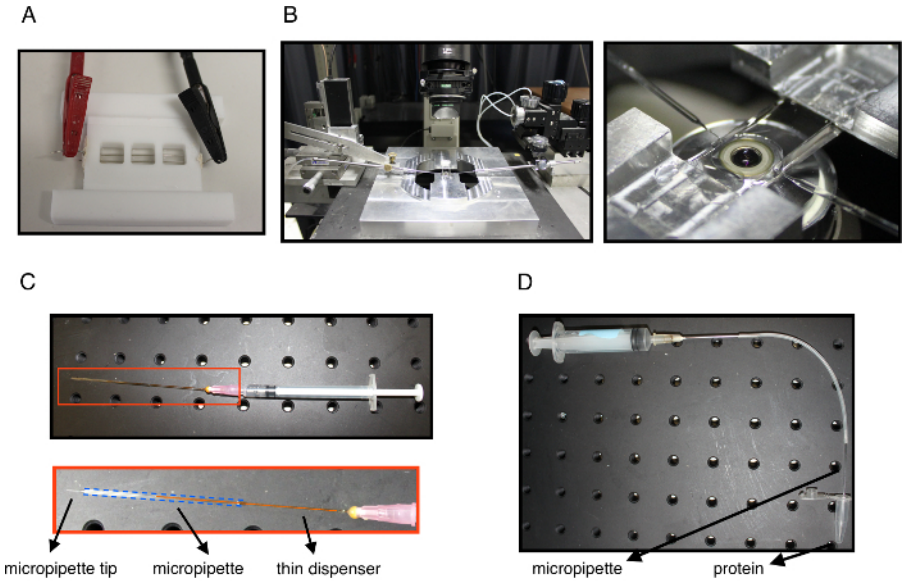

Figure 1: Experimental setup. (**A**) The GUV electroformation chamber with electrical connectors attached to Pt-wires. (**B**) Left: the experimental system showing the microscope, the experimental chamber above the objective and two micropipettes (left and right) attached to the micromanipulators and inserted into the experimental chamber for tube pulling and protein injection. Right: a close-up view of the experimental chamber mounted above the objective showing the tips of the aspiration and the injection micropipettes inserted. (**C**) A syringe equipped with a thin dispenser inserted into a micropipette at its back end. The bottom is a close-up view of the dispenser inside the micropipette with the blue dotted line outlining the micropipette. This system is used to fill the micropipette with casein to passivate the glass surface and also to back fill with mineral oil when needed. (**D**) A system used to aspirate µL quantities of the protein solution. The needle is connected to a syringe and to tubing which is connected to the injection micropipette. The micropipette tip is carefully immersed into the protein solution and aspirated so to fill the micropipette tip. The micropipette is then back filled with mineral oil using the system shown in panel C. Please click here to view a larger version of this figure.

A membrane nanotube, ranging in radius from 7 nm to several hundred nm, can be pulled from a GUV by an external force. This method was initially designed to measure the elastic properties of cell membranes and vesicles, such as the bending rigidity[15,16]. In most recent works, the method was extended to study the interaction of proteins with curved membranes by microinjecting the proteins near the pulled nanotube[7,17]. Other methods have been developed for studying membrane-curving proteins. In one method, proteins are incubated with differently sized liposomes tethered to a passivated surface. Confocal microscopy is used to measure the protein binding as a function of liposome diameter, which can indicate curvature-induced sorting[18,19]. In another method, proteins are injected near a micro-aspirated GUV to measure their ability to spontaneously induce tubules[20,21]. The method described in this protocol is uniquely suited to study membrane-curving proteins involved in endocytosis, where most proteins typically encounter preformed membrane nanotubes connecting the cargo-containing membrane invagination with the underlying flat plasma membrane. Furthermore, in this method, unlike in the assay with tethered small liposomes, the membrane nanotube is continuously connected to the membrane; therefore, it is in mechanical equilibrium with the GUV, a situation expected *in vivo*. Hence, fundamental membrane physics applies and we can infer a plethora of mechanical properties from our measurements[22,23,24].

For a full implementation of this method, the necessary equipment includes a confocal microscope, optical tweezers, and one or two micropipettes connected to a water tank (**Figure 1B**). By combining all three, it is possible to simultaneously measure membrane tension, membrane curvature, surface density of proteins, and tube force[25]. Micropipette aspiration is essential and it is easily constructed by inserting a glass micropipette into a holder connected to a water tank, which, via hydrostatic pressure, controls the aspiration pressure[26]. The micropipette and the holder are controlled by a micromanipulator and, ideally, in one direction by a piezo-actuator for precision movement. To pull a nanotube, the microaspirated GUV is briefly stuck to a micron-sized bead then pulled away creating a nanotube. In this implementation, the bead is held by optical tweezers, which can be constructed by following a published protocol[27]. It is possible to dispense of the optical tweezers and pull nanotubes in different ways, although at the cost of accurate force measurements. If it is too challenging to build an optical trap or if force measurements are not essential, such as if one simply wants to check the preference of proteins for curved membranes, a tube can be pulled using a bead aspirated at the tip of a second micropipette[28]. It is also possible to pull tubes using gravitational force[29] or flow[30,31]. Furthermore, confocal microscopy is not essential either; however, it is preferred so to measure the surface density of proteins. It also allows measuring the nanotube radius from fluorescence intensity of lipids in the tube, thus independently of membrane force and tension. Inferring tube radius from fluorescence is particularly important if the relationship between these quantities deviates from well-established equations due to the presence of membrane-adhered proteins[25]. Importantly, one cannot dispense of both the optical trap and confocal microscopy, as it will not be possible to measure the tube curvature.

The method as described in this protocol has been used to study the curvature-induced sorting of various peripheral membrane proteins on nanotubes, mostly those from the BAR family[25,32,33,34]. It was also shown that the conically shaped transmembrane potassium channel KvAP is enriched on curved nanotubes in the same way as BAR proteins[35]. By optimizing the method to encapsulate proteins inside GUVs, the interaction of proteins with negative curvature has been recently investigated as well[36]. Furthermore, this method has been used to elucidate the formation of protein scaffolds[25,37] and to study the mechanism of membrane scission by either line tension[38], protein dynamin[39], or by BAR proteins[40,41]. In addition to proteins, small molecules or ions can also induce curvature. Using this method, calcium ions were shown to induce positive curvature under salt-free conditions[42]. Interestingly, it has also been shown that lipids can undergo curvature sorting, although only for compositions that are near a demixing point[43,44]. In sum, the method can be used by researchers interested in investigating how either integral membrane components (*e.g.*, lipids or transmembrane proteins) or peripherally binding molecules (either inside or outside GUVs) interact with cylindrically curved membranes, from mechanical and quantitative points of view. It is also intended for those interested in measuring the mechanical properties of the membrane itself[22,23,45].

Protocol

1. Preparation of GUVs by Electroformation on Pt-wires

1. Clean the electroformation chamber (see **Introduction** and **Figure 1A**) and the Pt-wires with an organic solvent such as ethanol or acetone to wash away the lipids and with water to wash away the salts.
   NOTE: We suggest thoroughly wiping away the residue with ethanol-soaked tissue then sonicating in acetone, ethanol, then water, each for 5 min.
2. Prepare a lipid mix of a desired lipid composition at 1 mg/mL in chloroform. The mix should contain ~ 0.05% molar fraction of a lipid conjugated with biotin (*e.g.*, 1,2-distearoyl-sn-glycero-3-phosphoethanolamine-N-[biotinyl(polyethyleneglycol)-2000]) and ~ 0.5% molar fraction of a lipid conjugated with a fluorophore (*e.g.*, BODIPY-TR-C5-ceramide).
   NOTE: In our experience, it was difficult to produce GUVs at a high yield containing more than 30% charged lipids.
   CAUTION: Chloroform should be handled inside a chemical hood wearing appropriate gloves.
3. Insert a pair of Pt-wires into the electroformation chamber. Deposit the lipid mix onto the Pt-wires in drops separated by ~ 2-3 mm (total ~ 4 µL of the mix).
4. Dry the wires under vacuum for 30–60 min at room temperature.
5. Seal the bottom of the chamber by adhering the coverslip over the chamber using silicon grease. Fill the chamber with a buffered solution containing NaCl, sucrose, and a buffering agent (*e.g.*, 70 mM NaCl, 100 mM sucrose, and 10 mM Tris, at pH 7.4). This medium will be inside the GUVs in the experiment. It is essential that the osmolarity of this medium match the osmolarity of the experimental medium within ~ 10%. Use sucrose to adjust the osmolarity. Add proteins to the solution at a desired concentration if the goal is to encapsulate them in the GUVs.
   CAUTION: Various salts and sugars in the buffer can affect the bending rigidity and the spontaneous curvature of membranes[24,42,46,47].
6. Seal the top of the chamber by adhering a coverslip with silicon grease ensuring minimum air inside the chamber. Apply a sine AC current through the Pt-wires at 500 Hz and 280 mV.
   NOTE: The growth time and temperature must be optimized depending on the lipid composition and the sensitivity of the protein. When using natural lipid extracts, and also when encapsulating proteins in GUVs, the best yield was achieved by growing GUVs at 4 °C overnight. In the absence of proteins, and for synthetic lipid compositions, growth at room temperature for ~ 2 h was sufficient.

2. Preparation of the Experimental Chamber and the Micropipettes

1. To prepare micropipettes, pull a glass capillary using a pipette puller. It is suggested to use a glass capillary with internal and external radii of, respectively, 0.7 mm and 1 mm. Then, refine the tip of the micropipette so that its inner diameter is 5–7 µm, by using a microforge. If proteins or other molecules will be injected in the experiment, pull another micropipette and refine its tip to a inner diameter of 8–15 µm.
2. Construct an experimental chamber by placing two rectangular microscopy coverslips onto a metallic base as shown in **Figure 1**. The coverslips should be separated by ~ 1 mm. The chamber should have openings along the long edges (see **Figure 1**). The open sides should fit the tip of the micropipette where the tip should reach at least the center of the chamber.
3. Prepare the experimental buffer whose osmolarity should not differ by more than 10% from the buffer used to grow GUVs. Adjust the osmolarity with glucose. An example of an experimental buffer that was used in studying the interaction of endophilin with nanotubes is 100 mM NaCl, 40 mM glucose, buffered with Tris to pH 7.4. A combination of sucrose inside/glucose outside ensures: (a) sufficient phase contrast to observe GUVs with bright field microscopy, and (b) higher density inside the GUVs which causes them to settle on the bottom of the chamber. Adjust salt concentration based on experimental requirement.
   NOTE: In addition to affecting the membrane's mechanical properties, in our experience, high glucose concentration (> 300 mM) negatively affects the establishment of streptavidin-biotin bonds, required to pull a nanotube. Furthermore, too little salt inhibits streptavidin-biotin bonds, while too high of a concentration screens protein-membrane interactions. In case of protein encapsulation, using very high salt concentration in the external buffer (*e.g.*, >200 mM NaCl) can be used as a trick to detach the proteins from the outer leaflet[36]. It is necessary to experiment with a range of salt concentration to find the optimal binding conditions of the molecule of interest.
4. **30–60 min before collecting GUVs for the experiment, passivate the glass surfaces by filling both the experimental chamber and the aspiration micropipette with a 5 mg/mL solution of a highly pure β-casein (*e.g.*, dissolved in the experimental buffer). β-casein creates a protective layer on the glass surfaces, preventing GUVs to adhere too strongly, which would cause them to burst. Incubate with β-casein for 30–60 min.**
   NOTE: There should be no bubbles inside the micropipette that would interfere with controlling membrane tension.
   1. To build a dispenser for filling micropipettes, break a syringe needle close to the plastic connector and glue into it a thin silica capillary (such as those used for liquid chromatography) (**Figure 1C**).
5. During incubation with β-casein, mount the chamber on the microscope and center it above the objective. Insert the tip of the aspiration micropipette through the opening along the long edge and bring the tip above the microscope objective. Adjust the water tank level so that the aspiration pressure is near zero (there should be no heavy flow in or out of the pipette, which can be seen under the microscope).

6. **In case the proteins or other molecules will be injected during the experiment, fill the injection micropipette with the desired molecule dissolved in the experimental buffer at a concentration of choice, mount the micropipette inside a micromanipulator, and insert through the opposite side of the experimental chamber.**
    1. To use a minimum amount of proteins, fill only the micropipette tip with the protein by aspiration. To do that, wrap the end of a needle attached to a syringe with plastic tubing. Insert the tubing into the back of the injection micropipette.
    2. Very carefully immerse the tip of the micropipette into the protein solution and aspirate it to fill the tip of the micropipette.
    NOTE: This simple setup is shown in **Figure 1D** and, in our experience, it allows aspirating from as little as a few µL of the protein solution.
    3. Backfill the rest of the injection micropipette with mineral oil to prevent mixing of the protein solution and the water from the water tank (using the setup in **Figure 1C**).
    4. Take care not to introduce air bubbles into the injection pipette, as it will induce unstable injection pressure. Alternatively, if the protein quantity is sufficient, fill the micropipette with the proteins the same way as filling with β-casein as described in step 2.4. Adjust the water tank level to minimize the aspiration pressure in the injection pipette.
    NOTE: The concentration of the injected molecule or ion near the nanotube is going to be lower due to dilution and it can be estimated by measuring the fluorescence intensity decrease as a function of the distance from the pipette exit[42]. It is however more important to know the bilayer-bound density of the injected molecule, which can be precisely measured (see Section 4).

7. After incubation with β-casein, remove the solution from the chamber, and rinse with the experimental buffer several times. Fill with the experimental buffer.
8. Stop electroformation of GUVs and collect them directly from the Pt-wires. Add a few µL of the GUV solution to the experimental chamber. Use only freshly prepared GUVs.
9. Add a few µL of streptavidin-coated beads to the experimental chamber to a final concentration of beads in the chamber at around 0.1 x 10^{-3} % (w/v) or less. Polystyrene beads ~3 µm in diameter are recommended (polystyrene beads in water have a near-optimal refractive index contrast with regards to maximizing the gradient force with respect to the scattering force in the optical trap). The bead concentration can be adjusted based on the experiment: a very low concentration makes it difficult to find them in the chamber, and a too high concentration runs the risk of multiple beads falling into the optical tweezers.

3. Pulling a Membrane Nanotube from a GUV

1. Let the GUVs and the beads settle to the bottom of the chamber. Deflate the GUVs by letting a little of the experimental buffer evaporate, for approximately ~ 15 min. Deflating the GUVs is essential to produce some excess area that can be aspirated with the micropipette. GUVs should visibly undulate (*i.e.*, appear floppy) under the light microscope. If they appear tense, allow for more evaporation time.
NOTE: The osmolarity change rate depends on the evaporating surface area, the temperature, *etc.*, and should be closely monitored. In principle, the osmolarity difference could be set from start by adjusting the sucrose/glucose concentration, however, care should be taken not to induce an osmotic shock.
2. Find a floppy GUV and aspirate it into the pipette. The length of the aspiration tongue (the part of the membrane inside the pipette) should be equal to or larger than the pipette radius for the theoretical analysis to be applicable[15,16,22,23] (**Figure 2**). Try several GUVs. If none of the GUVs can be aspirated to produce a long enough tongue, wait a few more minutes. If GUVs are floppy enough, proceed to the next step.
3. Seal the chamber with mineral oil, to prevent further evaporation of the buffer. Do so by carefully pipetting the oil along the open edges of the experimental chamber.
4. To set the zero position of the aspiration pressure, first, look for a bead in the chamber and position the aspiration pipette exit near the bead. Adjust the height of the water tank so that the bead is neither sucked in nor blown away by the aspiration pipette. Although the mineral oil prevents evaporation and therefore further pressure changes inside the chamber, zero the aspiration pressure before measuring each GUV.
5. Find a GUV and aspirate it. Move the micropipette up and out of focus (to keep the GUV away from the surface where it might be pulled out of the pipette by shear stress when the chamber is moved).
6. Look for a bead by carefully moving around the chamber. Sudden moves can eject the GUV. Trap it with optical tweezers at a distance ~ 20 µm away from the chamber bottom. Ensure that the region of interest is clean with no other beads or membranes in sight. Anything falling in the optical tweezers other than the bead will disrupt the measurement.
7. Bring the GUV back into focus, and away from the bead with the micropipette aligned with the optical trap (**Figure 2**).
8. Record the movement of the bead for 1–2 min to measure the equilibrium position (required for force measurements).
9. Reduce the pressure inside the micropipette as much as possible without losing the GUV so to decrease the membrane tension. Carefully bring the GUV in contact with the bead for around a second, establishing streptavidin-biotin bonds, then gently pull back creating a nanotube. The motion of the GUV toward or away from the bead should ideally be done with a piezo-actuator to minimally disrupt the bead in the optical tweezers.
NOTE: If the nanotube does not form, it could be due to poor streptavidin coating of the bead, insufficient amount of biotinylated lipids in the GUV, insufficient concentration of salt or excessive concentration of glucose in the experimental buffer, or the membrane tension in the GUV is too high[48].
10. Increase the aspiration pressure so to recreate the aspiration tongue. Align the tube to lie in the axis of the aspiration pipette and maximally focus on the tube (**Figure 2**).
11. Ensure that the GUV equator and the tube are in focus. Record the movement of the bead with bright field microscopy for a few min (here, the camera acquisition speed is 30 Hz). Record the height, *h*, of the water tank with respect to the zero position. Take a few confocal images of the system (**Figure 2**).
12. Repeat the previous step at different aspiration pressures, implicitly membrane tensions.Typical tension range is 0.015–0.2 mN/m, with a step size of around 0.02 mN/m.
13. If injecting proteins or molecules near the system, bring the injection micropipette near the nanotube, making sure that the bead in the optical trap is not perturbed. Gently inject at a pressure of around 1–2 Pa.
14. **After the protein binding has equilibrated (the fluorescence intensity of the injected protein on the membrane remains constant on the GUV), repeat the step-wise measurements as with the bare membrane (steps 3.11 and 3.12).**

NOTE: Since the measurements are performed while injecting proteins near the GUV at constant pressure, the bulk concentration of the protein remains roughly unchanged near the GUV; thus, protein desorption should be negligible during the measurement.

1. Alternatively, it is possible to incubate the GUVs together with the proteins before performing tube-pulling experiments to ensure a constant protein bulk concentration. Given that the relative membrane fraction of proteins on the tube and on the GUV is measured, the way proteins are delivered does not influence the curvature-sorting calculation (see Section 4).

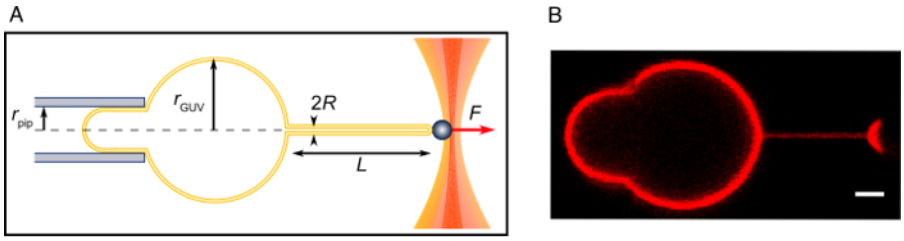

Figure 2: Tube-pulling experiment. (**A**) Schematics of the experiment. (**B**) A confocal image of a pulled tube as described in this Protocol. Scale bar = 2 µm. Please click here to view a larger version of this figure.

4. Measurements and Data Analysis

1. **Measuring membrane tension**
   1. Calculate the hydrostatic pressure for each step at constant aspiration pressure:
      $\Delta P = pgh$
      where p is the water density, g gravitational acceleration, and h the height of the water tank from step 3.11.
   2. From confocal images, measure the radius of the GUV, r_{GUV}, and the radius of the aspiration pipette, r_{pip} (**Figure 2**).
   3. Calculate the membrane tension, σ, using Laplace's equation[49]:
      $$\sigma = \Delta P \frac{r_{pip}}{2(1-r_{pip}/r_{GUV})}$$

2. **Measuring membrane force**
   1. Determine the stiffness of the optical tweezers, k, by using one of several calibration methods[27]. In this setup, measure k using the viscous drag method[27].
   2. Calculate the equilibrium position of the bead, a_0, as an average from a measurement before pulling the tube (step 3.8).
   3. For each constant tension measurement, calculate the equilibrium membrane force, F, from Hooke's law:
      $F = k(a - a_0)$
      where a is the average position of the bead during that measurement.

3. **Measuring tube radius**
   1. In the case of a bare membrane (no added membrane-curving molecules), calculate the tube radius, R, from the force as:
      $R = F/(4\pi\sigma)$
      (references[22,23]).
   2. To measure the tube radius in the presence of membrane-curving molecules and independently of step 4.3.1, first, record the lipid fluorescence intensity along the tube length, I_{tub}, and along the GUV contour, I_{GUV}. Measure the average fluorescence intensity of a fluorophore in or bound to the membrane as an average intensity along the brightest line of a tube or a GUV contour. Select a rectangular box containing a horizontal section of the GUV contour or the tube and calculate the sum of the fluorescence intensities of each horizontal line in the box.
      1. Divide each sum by the number of pixels of the horizontal line (*i.e.*, the box width). Note that in the selected box, there should be no other membranes present. The fluorescence intensity profile along the length of the selected box is obtained.
      2. After subtracting the background intensity, take the average pixel fluorescence intensity from the brightest line. The tube radius is linearly related to the ratio of fluorescence along the contour of the tube and of the GUV as:
         $R = K_{tub} I_{tub}/I_{GUV}$
         where K_{tub} is a calibration factor[25].
         NOTE: This method can be used to measure the tube radius in the 10–80 nm range (when the tube is narrow enough to lie within one confocal voxel width) and with a somewhat greater uncertainty in the 80 nm and higher range. The sensitivity of the measurement depends on the setup.
   3. Determine K_{tub} by performing independent radius measurements in steps 4.3.1 and 4.3.2 on a simple membrane composition using uncharged lipids. Such simple membrane composition ensures that the radius and the force have the simple relationship given in step 4.3.1. Repeat the experiment several times and plot R, deduced from the force (step 4.3.1) versus I_{tub}/I_{GUV} (step 4.3.2). Calculate K_{tub} from the fit. In this setup, K_{tub} = 200 ± 50 nm by using egg L-α-phosphatidylcholine (egg-PC) membrane and a fluorescent lipid whose fluorescence minimally depends on polarization[25].
      NOTE: K_{tub} must be measured for different objectives, due to their different confocal voxel volumes. The lipid fluorophore should not interact with the injected proteins/molecules. The fluorescent lipid recommended here, BODIPY TR ceramide, is not expected to have any interactions with the proteins. This assumption was confirmed with previous studies of BAR and I-BAR domains[25,36,37], which have shown that at high protein surface coverage, the tube radius is fixed by the proteins, regardless of the tension in the GUV. If proteins interact with the lipid fluorophore, a depletion or enrichment of the fluorophore will be observed in the tube at varied high protein surface fractions.

4. **Measuring the surface density of proteins**
    1. Prepare lipid mixes using a simple uncharged lipid (*e.g.*, egg-PC) supplemented with about five different mole fractions of a fluorescent lipid (of the same wavelength as the dye used to label the protein, *e.g.*, BODIPY-FLC5-hexadecanoyl-phosphatidylcholine (HPC*) for *e.g.*, the Alexa488-labeled protein) in the range: X_{HPC^*} = 0.01–1%. Prepare GUVs in 100 mM sucrose by electroformation on ITO plates (follow step 1 of a previous publication[13]).
    2. Collect GUVs and transfer to an experimental chamber passivated with β-casein. Use *e.g.*, 100 mM glucose for the experimental solution. Wait a few minutes for the GUVs to settle.
    3. Take confocal fluorescence images of GUVs and record the average fluorescence intensity along the GUV contours as a function of the mole fraction of the fluorescent lipid (see Step 4.3.2). For each composition, calculate the area density of the fluorescent lipid, φ_{HPC^*}. For example, by assuming that the area per lipid is 0.7 nm^2, φ_{HPC^*} = 1.43 x 10^6 X_{HPC^*} per leaflet. Plot HPC* fluorescence intensity in the GUV, $I_{HPC^*,GUV}$, *versus* φ_{HPC^*}. Fit gives the calibration constant, *A*, given by $\varphi_{HPC^*} = AI_{HPC^*,GUV}$. *A* depends on the microscopy settings, such as the laser power and the detector sensitivity (*i.e.*, gain), therefore record *A* for various commonly used microscopy settings (see example in **Figure 3**).
    4. Prepare several solutions of HPC* dissolved in detergent, *e.g.*, sodium dodecyl-sulfate (SDS), at different concentrations in the range from ~ 1 to 10-50 µM. Record fluorescence intensity of each solution in bulk and calculate the slope of intensity *versus* concentration (**Figure 3**). Repeat the measurement with the fluorophore that will be conjugated to the protein in a similar concentration range (see the example with Alexa488 in **Figure 3**). This measurement is required to relate the fluorescence intensities of the protein label and the lipid label, $I_{A488,bulk}$ / $I_{HPC^*,bulk}$, as they may not necessarily emit in the same way at the same bulk concentration.
    5. Measure the number of fluorophores per protein molecule using a fluorospectrometer. For example, for the case of Alexa488, the number of Alexa488 molecules per protein, n_{A488}, can be calculated using the following relation:
    $n_{A488} = (A_{494}/\varepsilon_{A488})/((A_{280} - 0.11A_{494}) / \varepsilon_{prot})$
    where A_{494} and A_{280} are the absorbance values per unit length at 494 nm and 280 nm, respectively, and ε_{A488} and ε_{prot} are the molecular absorption coefficients of Alexa488 and the protein, respectively.
    6. Calculate the surface density of the protein on the GUV, $\varphi_{prot,GUV}$, according to the following formula:
    $$\varphi_{\mathrm{prot,GUV}} = \frac{AI_{\mathrm{A488,GUV}}}{n_{\mathrm{A488}} I_{\mathrm{A488,bulk}} / I_{\mathrm{HPC^*,bulk}}}$$
    Keep in mind the polymerization state of the protein. For example, BAR proteins dimerize, therefore the calculated density will be that of the BAR monomer per area if using the extinction coefficient of the monomeric form.

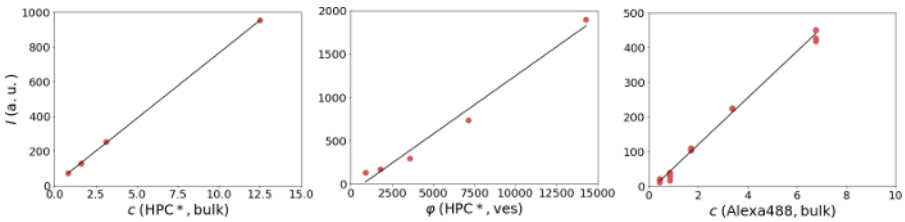

Figure 3: An example of protein surface density calibration. Measured are the HPC* lipid fluorescence intensity in bulk (left) and in GUVs (center). Also, measured are the bulk fluorescence intensity of Alexa488 (bound to a BAR domain) (right). Fluorescence intensity linearly scales with concentration. Measurements shown are for specific detection gain and laser power output. Plots generated based on data from reference[37]. Please click here to view a larger version of this figure.

Representative Results

The tube-pulling experiment can give vital mechanical information about the membrane. In the absence of proteins or other molecules that couple with membrane curvature, the membrane force and tube radius can be related with membrane tension by applying the Canham-Helfrich Hamiltonian equation to a tube pulled from a GUV[50,51]

$$\mathcal{F} = \frac{\kappa}{2}\left(\frac{1}{r} - \frac{1}{R_0}\right)^2 A + \sigma A - fL \quad \textbf{(Equation 1)}$$

where $\mathcal{F}$ is the membrane free energy of the tube, *K* membrane bending rigidity, *r* and R_0 are, respectively, the mean and the spontaneous radii of curvature, σ membrane tension, *A* the area of the tube, *L* the length of the tube, and *f* the point force exerted by the tube on the bead. At equilibrium, *r* is the tube radius, denoted as *R*, and *f* becomes the tube-retraction force, *F*, *i.e.*, the equilibrium force by which the tube is pulling the bead in the optical trap. To compute *F* and *R*, we minimize $\mathcal{F}$ with respect to *L* and *r*, yielding[22,23]

$$F = 2\pi\sqrt{2\sigma\kappa + \frac{\kappa^2}{{R_0}^2}} - 2\pi\kappa\frac{1}{R_0} \quad \textbf{(Equation 2)}$$

$$\frac{1}{R^2} = \frac{2\sigma}{\kappa} + \frac{1}{{R_0}^2} \quad \textbf{(Equation 3)}$$

R_0 is neglected if both leaflets of the membrane have the same composition, although it is speculated that other factors, such as charge repulsions can induce some spontaneous curvature[42]. Force and radius measurements on tubes pulled from 100% DOPC GUVs are in excellent agreement with theoretical predictions in **Equation 2** and **Equation 3** (**Figure 4**). The two measurements are independent as the force is measured from the displacement of the bead in the optical trap and the radius from fluorescence intensity, therefore providing two ways of calculating the membrane bending rigidity. Fitting **Equation 2** and **Equation 3** to the shown data yields: K = (25.1 ± 1.4) (mean ± SD) k_BT and (22.1 ± 1.5) k_BT, respectively, as previously measured[42].

If experimenting with curvature-coupling proteins, it is suggested to use the more sophisticated Hamiltonian's equation than the one in **Equation 1**, as **Equation 1** only accounts for an effective spontaneous curvature and does not account for the effect of proteins on the membrane's mechanical properties or possible protein-protein interactions. See, *e.g.*,[25,35,36,52,53]. Although advanced theoretical models are essential for an in-depth understanding of a specific protein-membrane system, without resorting to them, it is still possible to obtain very useful information from the tube-pulling method.

For example, to test if proteins sense curvature, the relative intensity of proteins on the tube is measured compared to the GUV, which is considered flat. The interaction with positive curvature is studied by injecting the proteins near the tube with the second micropipette[25]. The interaction with negative curvature or the behavior of transmembrane proteins is studied by encapsulating or reconstituting proteins during GUV formation[35,36]. The relative enrichment of BAR and KvAP proteins on membrane tubes over the underlying GUVs indicates that they prefer curved membranes (**Figure 5**). To be more quantitative, this enrichment may be calculated as a sorting coefficient, S, according to:

$$S = \frac{I_{\text{prot,tub}}/I_{\text{prot,GUV}}}{I_{\text{lip,tub}}/I_{\text{lip,GUV}}} \quad \textbf{(Equation 4)}$$

where $I_{\text{prot,tub}}$ and $I_{\text{prot,GUV}}$ are the fluorescence intensities of proteins on the tube and on the GUV, respectively, and $I_{\text{lip,tub}}$ and $I_{\text{lip,GUV}}$ are the fluorescence intensities of lipids on the tube and on the GUV, respectively.

Another example is measuring the tube force as the protein binds to the membrane. **Figure 5B**,C shows that an N-BAR protein endophilin A2 gradually reduces the tube force, decreasing it to zero, indicating that it has formed a three-dimensional structure that keeps the tube stable, which is termed a scaffold. Such structures play important roles in endocytosis, by fixing the tube radius but also in enabling scission[7,41]. Measurement of S, as well as the mechanical and morphological effects that proteins impose on membranes provides important insights into how they operate in the membrane-bending phenomena in the cell.

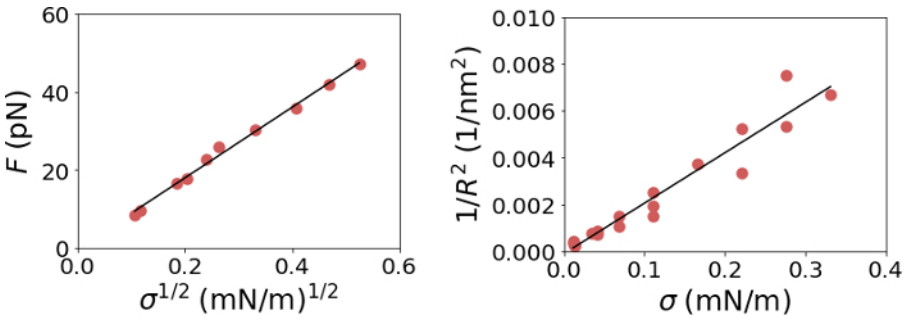

Figure 4: Representative results of mechanical measurements in the absence of proteins. Shown are linearized force and tube radius dependence on membrane tension for a 100% DOPC membrane, from three independent measurements, published previously[42]. Please click here to view a larger version of this figure.

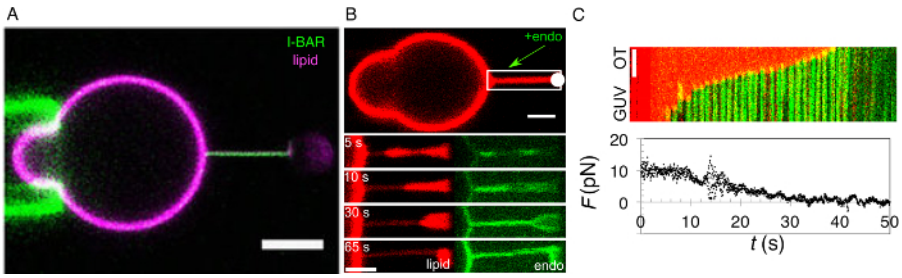

Figure 5: Representative results of curvature sensing and scaffold formation by BAR proteins. (**A**) Curvature sensing by the I-BAR protein IRSp53. The protein senses negative membrane curvature and is bound on the inside of the GUV, with negligible amount of protein present on outer membrane leaflet. Scale bar = 5 µm. Reprinted from[36], under the Creative Commons CC-BY license, Copyright 2015, Nature Publishing Group. (**B**) Forming a protein scaffold by the N-BAR protein endophilin. Proteins are injected near the tube and are therefore bound on the outer membrane leaflet. As described in[37], endophilin binds to the tube's base and forms a scaffold that continuously grows along the tube from the GUV toward the optical trap (OT, white circle). (**C**) A kymogram of endophilin scaffold growth from the GUV to the bead, with the lipid and protein channels overlaid. The plot shows tube force, F, as a function of time, t. The timescales in the kymogram and the plot are the same (x-axis is shared). In *B* and *C*, Scale bar = 2 µm. Reprinted with permission from reference[37], Copyright (2016) National Academy of Sciences. Please click here to view a larger version of this figure.

Discussion

The method of pulling tubes from GUVs gives rich information on the membrane-protein system, as it is not only the means to measure the fundamental mechanical properties of the membrane, but it helps to shed light on the coupling between proteins and membrane curvature. As discussed in the Introduction, other techniques exist to measure the effects of membrane-curving proteins, either by incubating the proteins with sub-micron liposomes tethered to a passivated surface[18,19] or by observing the spontaneous formation of tubules in micropipette-aspirated GUVs upon the injection of a protein[20,21]. The method described here provides direct geometric connection to endocytosis and is unique in providing the important physical measurements of the system at the same time, such as protein density, membrane tension, and membrane force.

An important limitation of the method is that it is not trivial to construct and calibrate all the components involved in the assay. However, while a combination of confocal microscopy, optical tweezers, and micromanipulation provides maximal information, some components can be substituted as discussed in the Introduction, depending on the information that needs to be learned about the system. The minimal components required to successfully probe the curvature coupling of a protein, or any other potential curvature-coupled molecule, are a micropipette aspirator and a confocal microscope, with the optical tweezers being dispensable. Importantly, many of the calibrations (such as the calibration for membrane tube radius and for determining protein surface density) are typically only needed to be performed once. Another limitation of the method is that it can measure only one GUV at a time, amounting to two to three GUVs per hour (with practice); however each measurement provides a wealth of data.

For higher throughput measurements or if it is essential to study the interaction of proteins with spherical and not tubular geometries, other assays will need to be explored or developed. Future efforts will be devoted to: (1) designing a higher-throughput system in which multiple tubes (from multiple GUVs) could be pulled and measured at the same time, and (2) integrating super-resolution microscopy so to study the details of the protein scaffold that forms on the nanotubes.

Disclosures

The authors have nothing to disclose.

Acknowledgements

The authors thank Benoit Sorre, Damien Cuvelier, Pierre Nassoy, François Quemeneur, and Gil Toombes for their essential contributions to establish the nanotube method in the group. The P.B. group belongs to the CNRS consortium CellTiss, to the Labex CelTisPhyBio (ANR-11-LABX0038), and to Paris Sciences et Lettres (ANR-10-IDEX-0001-02). F.-C. Tsai was funded by the EMBO Long-Term fellowship (ALTF 1527-2014) and Marie Curie actions (H2020-MSCA-IF-2014, project membrane-ezrin-actin). M.S. is a Junior Fellow of the Simons Society of Fellows.

References

1. McMahon, H. T., & Gallop, J. L. Membrane curvature and mechanisms of dynamic cell membrane remodelling. *Nature.* **438** (7068), 590-596 (2005).
2. Johannes, L., Wunder, C., & Bassereau, P. Bending "on the rocks"--a cocktail of biophysical modules to build endocytic pathways. *Cold Spring Harb Perspect Biol.* **6** (1) (2014).
3. Dawson, J. C., Legg, J. A., & Machesky, L. M. Bar domain proteins: a role in tubulation, scission and actin assembly in clathrin-mediated endocytosis. *Trends Cell Biol.* **16** (10), 493-498 (2006).
4. Mim, C., & Unger, V. M. Membrane curvature and its generation by BAR proteins. *Trends Biochem Sci.* **37** (12), 526-533 (2012).
5. Qualmann, B., Koch, D., & Kessels, M. M. Let's go bananas: revisiting the endocytic BAR code. *EMBO J.* **30** (17), 3501-3515 (2011).
6. Rao, Y., & Haucke, V. Membrane shaping by the Bin/amphiphysin/Rvs (BAR) domain protein superfamily. *Cell Mol Life Sci.* **68** (24), 3983-3993 (2011).
7. Simunovic, M., Voth, G. A., Callan-Jones, A., & Bassereau, P. When Physics Takes Over: BAR Proteins and Membrane Curvature. *Trends Cell Biol.* **25** (12), 780-792 (2015).
8. Safari, F., & Suetsugu, S. The BAR Domain Superfamily Proteins from Subcellular Structures to Human Diseases. *Membranes (Basel).* **2** (1), 91-117 (2012).
9. Angelova, M. I., Soléau, S., Méléard, P., Faucon, F., & Bothorel, P. in *Trends in Colloid and Interface Science VI* Vol. 89 *Progress in Colloid & Polymer Science.* eds C. Helm, M. Lösche, & H. Möhwald) Ch. 29, 127-131 Steinkopff (1992).
10. Meleard, P., Bagatolli, L. A., & Pott, T. Giant unilamellar vesicle electroformation from lipid mixtures to native membranes under physiological conditions. *Methods Enzymol.* **465** 161-176 (2009).
11. Montes, L. R., Alonso, A., Goni, F. M., & Bagatolli, L. A. Giant unilamellar vesicles electroformed from native membranes and organic lipid mixtures under physiological conditions. *Biophys J.* **93** (10), 3548-3554 (2007).
12. Mathivet, L., Cribier, S., & Devaux, P. F. Shape change and physical properties of giant phospholipid vesicles prepared in the presence of an AC electric field. *Biophys J.* **70** (3), 1112-1121 (1996).
13. Collins, M. D., & Gordon, S. E. Giant liposome preparation for imaging and patch-clamp electrophysiology. *J Vis Exp.* (76) (2013).
14. Garten, M., Aimon, S., Bassereau, P., & Toombes, G. E. Reconstitution of a transmembrane protein, the voltage-gated ion channel, KvAP, into giant unilamellar vesicles for microscopy and patch clamp studies. *J Vis Exp.* (95), 52281 (2015).
15. Hochmuth, R. M., & Evans, E. A. Extensional flow of erythrocyte membrane from cell body to elastic tether. I. Analysis. *Biophys J.* **39** (1), 71-81 (1982).

16. Hochmuth, R. M., Wiles, H. C., Evans, E. A., & McCown, J. T. Extensional flow of erythrocyte membrane from cell body to elastic tether. II. Experiment. *Biophys J.* **39** (1), 83-89 (1982).
17. Bassereau, P., Sorre, B., & Levy, A. Bending lipid membranes: experiments after W. Helfrich's model. *Adv Colloid Interface Sci.* **208** 47-57 (2014).
18. Hatzakis, N. S. *et al.* How curved membranes recruit amphipathic helices and protein anchoring motifs. *Nature chemical biology.* **5** (11), 835-841 (2009).
19. Bhatia, V. K. *et al.* Amphipathic motifs in BAR domains are essential for membrane curvature sensing. *EMBO J.* **28** (21), 3303-3314 (2009).
20. Shi, Z., & Baumgart, T. Membrane tension and peripheral protein density mediate membrane shape transitions. *Nat Commun.* **6** 5974 (2015).
21. Chen, Z., Shi, Z., & Baumgart, T. Regulation of membrane-shape transitions induced by I-BAR domains. *Biophys J.* **109** (2), 298-307 (2015).
22. Cuvelier, D., Derenyi, I., Bassereau, P., & Nassoy, P. Coalescence of membrane tethers: experiments, theory, and applications. *Biophys J.* **88** (4), 2714-2726 (2005).
23. Derenyi, I., Julicher, F., & Prost, J. Formation and interaction of membrane tubes. *Phys Rev Lett.* **88** (23), 238101 (2002).
24. Dimova, R. Recent developments in the field of bending rigidity measurements on membranes. *Adv Colloid Interface Sci.* **208** 225-234 (2014).
25. Sorre, B. *et al.* Nature of curvature coupling of amphiphysin with membranes depends on its bound density. *Proc Natl Acad Sci U S A.* **109** (1), 173-178 (2012).
26. Evans, E., & Rawicz, W. Entropy-driven tension and bending elasticity in condensed-fluid membranes. *Phys Rev Lett.* **64** (17), 2094-2097 (1990).
27. Neuman, K. C., & Nagy, A. Single-molecule force spectroscopy: optical tweezers, magnetic tweezers and atomic force microscopy. *Nat Methods.* **5** (6), 491-505 (2008).
28. Capraro, B. R., Yoon, Y., Cho, W., & Baumgart, T. Curvature sensing by the epsin N-terminal homology domain measured on cylindrical lipid membrane tethers. *J Am Chem Soc.* **132** (4), 1200-1201 (2010).
29. Bo, L., & Waugh, R. E. Determination of bilayer membrane bending stiffness by tether formation from giant, thin-walled vesicles. *Biophys J.* **55** (3), 509-517 (1989).
30. Rossier, O. *et al.* Giant Vesicles under Flows: Extrusion and Retraction of Tubes. *Langmuir.* **19** (3), 575-584 (2003).
31. Borghi, N., Rossier, O., & Brochard-Wyart, F. Hydrodynamic extrusion of tubes from giant vesicles. *EPL (Europhysics Letters).* **64** (6), 837 (2003).
32. Zhu, C., Das, S. L., & Baumgart, T. Nonlinear sorting, curvature generation, and crowding of endophilin N-BAR on tubular membranes. *Biophys J.* **102** (8), 1837-1845 (2012).
33. Ramesh, P. *et al.* FBAR syndapin 1 recognizes and stabilizes highly curved tubular membranes in a concentration dependent manner. *Sci Rep.* **3** 1565 (2013).
34. Knorr, R. L. *et al.* Membrane morphology is actively transformed by covalent binding of the protein Atg8 to PE-lipids. *PLoS One.* **9** (12), e115357 (2014).
35. Aimon, S. *et al.* Membrane shape modulates transmembrane protein distribution. *Dev Cell.* **28** (2), 212-218 (2014).
36. Prévost, C. *et al.* IRSp53 senses negative membrane curvature and phase separates along membrane tubules. *Nat Commun.* (2015).
37. Simunovic, M. *et al.* How curvature-generating proteins build scaffolds on membrane nanotubes. *Proc Natl Acad Sci U S A.* **113** (40), 11226-11231 (2016).
38. Allain, J. M., Storm, C., Roux, A., Ben Amar, M., & Joanny, J. F. Fission of a multiphase membrane tube. *Phys Rev Lett.* **93** (15), 158104 (2004).
39. Morlot, S. *et al.* Membrane shape at the edge of the dynamin helix sets location and duration of the fission reaction. *Cell.* **151** (3), 619-629 (2012).
40. Renard, H. F. *et al.* Endophilin-A2 functions in membrane scission in clathrin-independent endocytosis. *Nature.* **517** (7535), 493-496 (2015).
41. Simunovic, M. *et al.* Friction Mediates Scission of Tubular Membranes Scaffolded by BAR Proteins. *Cell.* **170** (1) 172-184 (2017).
42. Simunovic, M., Lee, K. Y., & Bassereau, P. Celebrating Soft Matter's 10th anniversary: screening of the calcium-induced spontaneous curvature of lipid membranes. *Soft Matter.* **11** (25), 5030-5036 (2015).
43. Sorre, B. *et al.* Curvature-driven lipid sorting needs proximity to a demixing point and is aided by proteins. *Proc Natl Acad Sci U S A.* **106** (14), 5622-5626 (2009).
44. Heinrich, M., Tian, A., Esposito, C., & Baumgart, T. Dynamic sorting of lipids and proteins in membrane tubes with a moving phase boundary. *Proc Natl Acad Sci U S A.* **107** (16), 7208-7213 (2010).
45. Dasgupta, R., & Dimova, R. Inward and outward membrane tubes pulled from giant vesicles. *Journal of Physics D: Applied Physics.* **47** (28), 282001 (2014).
46. Vitkova, V., Genova, J., Mitov, M. D., & Bivas, I. Sugars in the aqueous phase change the mechanical properties of lipid mono- and bilayers. *Molecular Crystals and Liquid Crystals.* **449** 95-106 (2006).
47. Bouvrais, H. *Mechanical properties of giant vesicle membranes investigated by flickering technique.* University of Southern Denmark (2011).
48. Koster, G., Cacciuto, A., Derenyi, I., Frenkel, D., & Dogterom, M. Force barriers for membrane tube formation. *Phys Rev Lett.* **94** (6), 068101 (2005).
49. Kwok, R., & Evans, E. Thermoelasticity of large lecithin bilayer vesicles. *Biophys J.* **35** (3), 637-652 (1981).
50. Helfrich, W. Elastic properties of lipid bilayers: theory and possible experiments. *Z Naturforsch C.* **28** (11), 693-703 (1973).
51. Canham, P. B. The minimum energy of bending as a possible explanation of the biconcave shape of the human red blood cell. *J Theor Biol.* **26** (1), 61-81 (1970).
52. Marcerou, J. P., Prost, J., & Gruler, H. Elastic Model of Protein-Protein Interaction. *Nuovo Cimento Della Societa Italiana Di Fisica D-Condensed Matter Atomic Molecular and Chemical Physics Fluids Plasmas Biophysics.* **3** (1), 204-210 (1984).
53. Leibler, S. Curvature Instability in Membranes. *J Phys-Paris.* **47** (3), 507-516 (1986).

